Chin. Geogra. Sci. 2011 21(6) 656–665
doi: 10.1007/s11769-011-0505-x
www.springerlink.com/content/1002-0063

Fusion and Classification of Beijing-1 Small Satellite Remote Sensing Image for Land Cover Monitoring in Mining Area

DU Peijun[1, 2], YUAN Linshan[3], XIA Junshi[2], HE Jianguo[2]

(*1. Department of Geoinformatics, Nanjing University, Nanjing 210093, China; 2. Key Laboratory for Land Environment and Disaster Monitoring of SBSM, China University of Mining and Technology, Xuzhou 221116, China; 3. East China Mineral Exploration and Development Bureau, Nanjing 210007, China*)

Abstract: In order to promote the application of Beijing-1 small satellite (BJ-1) remote sensing data, the multispectral and panchromatic images captured by BJ-1 were used for land cover classification in Pangzhuang Coal Mining. An improved Intensity-Hue-Saturation (IHS) fusion algorithm is proposed to fuse panchromatic and multispectral images, in which intensity component and panchromatic image are combined using the weights determined by edge pixels in the panchromatic image identified by grey absolute correlation degree. This improved IHS fusion algorithm outperforms traditional IHS fusion method to a certain extent, evidenced by its ability in preserving spectral information and enhancing spatial details. Dempster-Shafer (D-S) evidence theory was adopted to combine the outputs of three member classifiers to generate the final classification map with higher accuracy than that by any individual classifier. Based on this study, we conclude that Beijing-1 small satellite remote sensing images are useful to monitor and analyze land cover change and ecological environment degradation in mining areas, and the proposed fusion algorithms at data and decision levels can integrate the advantages of multi-resolution images and multiple classifiers, improve the overall accuracy and produce a more reliable land cover map.

Keywords: grey absolute correlation degree; Intensity-Hue-Saturation (IHS) transformation; D-S evidence theory; Beijing-1 small satellite

Citation: Du Peijun, Yuan Linshan, Xia Junshi, He Jianguo, 2011. Fusion and classification of Beijing-1 small satellite remote sensing image for land cover monitoring in mining area. *Chinese Geographical Science*, 21(6): 656–665. doi: 10.1007/s11769-011-0505-x

1 Introduction

The continuous and excessive exploitation of underground coal mineral led to cumulative negative impacts on regional ecological environment and serious damage to land ecosystem. As the most advanced technique for dynamic monitoring of geographical phenomena and processes, remote sensing (RS) provides comprehensive, synthetic and timely data for monitoring land resources and ecological environment, which further contributes to regional sustainable development (Chen *et al*., 2004). Using remote sensing imagery to monitor ecological environment in mining areas has become a hot topic of environment remote sensing and digital mine building (Legg, 1990; Prakash and Gupta, 1998; Peng *et al*., 2002; Kiranmay, 2005; Silva *et al*., 2005). However, most of those studies used remote sensing imagery captured by Landsat TM/ETM+, SPOT, ASTER or other foreign sensors. In contrast, remote sensing images captured by Chinese satellites, for instance, Beijing-1 small satellite and HJ-1 small satellite, have not gotten wide uses in mining areas. It is worthy that we should attempt to promote the applications of such homemade remote sensing data to resources and environment monitoring in mining areas. Beijing-1 (BJ-1) small satellite, as one component of Disaster Monitoring Constellation (DMC),

Received date: 2010-09-10; accepted date: 2011-04-18
Foundation item: Under the auspices of National Natural Science Foundation of China (No. 40871195), Opening Fund of Beijing-1 Small Satellite Data Applications from State Key Laboratory for Remote Sensing Science (No. 200709), National High Technology Research and Development Program of China (No. 2007AA12Z162)
Corresponding author: DU Peijun. E-mail: dupjrs@126.com

was put into use in 2005 and has been widely used in many fields, such as urban planning, environmental protection, disaster monitoring and mitigation, land use and land cover (Fu *et al*., 2007; Mu *et al*., 2007; Wang *et al*., 2007; Rainer *et al*., 2010). Undoubtedly, resources and environment monitoring of mining areas can benefit from the experiences of these applications.

In order to promote such uses, it is necessary to conduct specific investigations to image processing algorithms according to the properties of selected data source. Image classification is an important procedure of remote sensing applications. For Beijing-1 small satellite images, it is necessary to combine the benefits of panchromatic image with 4 m resolution and multispectral images with 32 m resolution in order to exploit both spatial details and spectral discrimination capacity in classification process. Hence, fusion of panchromatic and multispectral images is of great importance. The performance of data fusion affects classification accuracy directly, further influences subsequent classification, thematic analysis, change detection and other processing operations.

In this paper, an improved IHS fusion algorithm based on grey absolute correlation degree and weighted summation of intensity component and panchromatic image is proposed to fuse the multi-resolution images of BJ-1 small satellite from data level, and D-S evidence theory is employed to combine the classification outputs of different classifiers from decision level. Pangzhuang Coal Mine, located in the northwestern Xuzhou City, is selected as the case study area to evaluate the usefulness of BJ-1 small satellite images to land cover and ecological environment monitoring in mining areas and design effective information extraction methods (for example, data fusion and classification) for practical applications. The research is expected to advance the applications of homemade BJ-1 small satellite remote sensing images to coal mining areas and demonstrate the advantages of BJ-1 panchromatic and multispectral image fusion algorithms at data and decision levels by a case study.

2 Improved IHS Fusion Algorithm

As the most popular fusion algorithm for multi-source remote sensing data, IHS fusion is able to preserve both high spatial resolution and fine spectral details in fused image by replacing the intensity component of multispectral images with high resolution image. But the spectral signature is always distorted because the intensity component is directly replaced by high resolution image, which results in difficulties in image recognition and classification. In order to overcome this limitation, the panchromatic image and intensity component can be added by specific weights to form a weighted intensity component, instead of direct replacement in standard IHS fusion process. For example, He *et al*. (2007) introduced grey correlation analysis to IHS fusion. In the process, edges were detected from high resolution synthetic aperture radar (SAR) image based on grey correlation degree at first, and the weight of intensity component was determined by edge information so as to combine the intensity component from multispectral images with high resolution SAR image more reliably; finally, inversed IHS transform was used to obtain fused data. This method can alleviate spectral distortion resulting from IHS transformation to an extent and obtain better results than traditional IHS fusion algorithm.

The key point for the improvement is detecting edge pixels based on grey system theory and assigning intensity and panchromatic image with different weights according to edge and non-edge pixels. As an effective theory for treating the uncertainties in inadequate data, small size of samples, incomplete information and devoid of experiences, grey system and grey correlation analysis have been widely used to edge detection, similarity measure and target identification (Deng, 1997; Lu *et al*., 2000; Ma *et al*., 2004; Zheng *et al*., 2004). Grey correlation analysis is based on correlation degree that measures the geometric relationship or similarity among different geometric curves represented by reference consequence and test consequence. If the shapes of two curves are quite similar, the correlation degree is high; and if the shapes are different from each other, the correlation degree is low. Based on this standard, edge pixels can be detected from panchromatic image.

2.1 Edge detection based on grey correlation analysis

Each pixel on the image must belong or not belong to the set of edge points. Edge pixels on an image are the set of pixels whose grey levels (or digital numbers, *DN*s) vary like a step or roof. The edge points are characterized by obvious changes of grey values among adjacent pixels, and grey correlation degree is a good indicator to

test this variation (Zheng *et al*., 2004). The idea of edge detection using grey correlation analysis is based on the fact that the grey level of an ideal non-edge point can be assumed identical with its immediate neighbors. For a pixel on the image, a test sequence is formed by the grey or *DN*s of its eight immediate neighbors and itself. This test sequence is then compared with a reference sequence consisting of the *DN*s of an ideal non-edge point and its immediate neighbors. The higher the correlation degree between the test sequence and reference sequence, the more similarity the two geometric shapes, so the pixel can be viewed as a non-edge point. Otherwise, low correlation degree means that the pixel is an edge point.

A lot of measures of correlation degree have been proposed and experimented (Mei, 1992; Li, 1995; Lu *et al*., 2000; Ma *et al*., 2004; He *et al*., 2007). Those measures can be categorized into three groups: distance-based correlation degree, slope-based correlation degree, and both distance-based and slope-based correlation degree. Among all those measures, grey absolute correlation degree based on distance is quite effective for edge detection owing to it advantages such as symmetry, uniqueness of correlation sequence, irrelevance to distance, operability and direction capacity (Mei, 1992). The detailed steps of calculating grey absolute correlation degree are as follows:

(1) Definition of reference and test sequences. Selecting the reference sequence as x_0 = [1, 1, 1, 1, 1, 1, 1, 1, 1] and test sequence as x_i = [$DN_{i,j}$, $DN_{i-1,j-1}$, $DN_{i-1,j}$, $DN_{i-1,j+1}$, $DN_{i,j-1}$, $DN_{i,j+1}$, $DN_{i+1,j-1}$, $DN_{i+1,j}$, $DN_{i+1,j+1}$]. where, i = 1, 2, …, M; j = 1, 2, …, N; and the grey of neighbors are assigned as the value of the pixel itself when i = 1, or j = 1, or i = M, or j = N.

(2) Normalization of test or reference sequences, aiming to make those sequences comparable.

$$x_0'(k) = x_0(k)/\overline{x}_0, \quad x_i'(k) = x_i(k)/\overline{x}_i \tag{1}$$

where $\overline{x}_0$ is the mean of reference sequence; $\overline{x}_i$ is the mean of test sequence; k is the number in the sequence, k = 1, 2, …, 9.

(3) Calculation of the correlation coefficient between the test and reference sequences $r(x_0'(k), x_i'(k))$, and corresponding grey absolute correlation degree $r(x_0', x_i')$.

$$r(x_0'(k), x_i'(k)) = \frac{1}{1+\left|(x_0'(k+1)-x_0'(k))-(x_i'(k+1)-x_i'(k))\right|} \quad (k = 1, 2, \ldots, 8) \tag{2}$$

$$r(x_0', x_i') = \frac{1}{8}\sum_{k=1}^{8} r(x_0'(k), x_i'(k)) \tag{3}$$

(4) Edge detection based on grey absolute correlation degree. If $r(x_0', x_i')$ is higher than a user defined threshold θ, the pixel is similar to the reference sequence and it is not viewed as an edge point; or else, the pixel is labeled as an edge point.

2.2 Improved IHS fusion based on edge information from grey absolute correlation degree

In order to overcome the spectral distortion in traditional IHS fusion algorithm, edge information extracted from high resolution panchromatic image based on grey absolute correlation degree is adopted to determine the weights of panchromatic image and intensity component in the procedures of IHS fusion. The improved fusion procedure consists of the following steps:

(1) IHS transformation to the three multispectral bands (Red, Green and Blue) to derive three components: I (Intensity), H (Hue) and S (Saturation) (Manfred *et al*., 2010).

(2) Edge detection from the panchromatic image based on grey absolute correlation degree, to form the sets of edge points and non-edge points. For edge pixels, the weight of panchromatic image is higher than that of intensity component on the corresponding image location in order to highlight the detailed structure information in the high resolution image; otherwise, the weight of intensity component is higher than that of panchromatic image in order to preserve the spectral signatures.

(3) Histogram matching of high resolution panchromatic image and I component, making the histogram of high resolution image similar to I component.

(4) Linear weighted summation of high resolution image and I component based on the weights derived from edge information. A new intensity component I′ is obtained by this operation. It can be described by:

$$\mathrm{I}'[i,j] = \omega_1[i,j] \times \mathrm{P}[i,j] + \omega_2[i,j] \times \mathrm{I}[i,j]$$

where, $\omega_2[i,j] = 1 - \omega_1[i,j]$; i, j represents the row and column number of a pixel.

(5) Inversed IHS transformation to the new intensity component I′, and retaining H (Hue) and S (Saturation) components, to derive three bands of new multispectral images fused with panchromatic image (Manfred *et al*., 2010).

The improved IHS fusion procedure is shown in Fig. 1.

3 Land Cover Classification Based on D-S Evidence Theory

D-S evidence theory is an advanced reasoning algorithm proposed by Dempster and improved by Shafer (Shafer, 1976; Li *et al*., 2007). It has been widely used to remote sensing image classification, information extraction and data fusion with great success (Liu *et al*., 2003; Wang *et al*., 2004; Foody *et al*., 2007; Manfred *et al*., 2010).

For a given recognition framework $\Theta = \{C_1, C_2, \ldots, C_N\}$ (N is the number of classes), a Basic Probability Allocation (BPA) function $m(\bullet)$: $2^{\Theta} \rightarrow [0, 1]$ should satisfy the following conditions:

$$m(\phi) = 0 \tag{4}$$

for all elements outside the framework

$$\sum_{A \subseteq \Theta} m(A) = 1 \tag{5}$$

for the probability of all elements belonging to Θ where, ϕ is the set of elements outside the framework; A, a nonempty subset of Θ, consists of several or all elements in Θ. In remote sensing image classification, $m(\bullet)$ works as a classifier.

Let B as a nonempty subset of Θ, and $A \subseteq B$, the belief function $Bel(\bullet)$, associated with the BPA function $m(\bullet)$, is used to assign a value in [0, 1] to every nonempty subset B of Θ. This value is called ′degree of belief in B′, defined by Equation (6) (Al-Ani and Deriche, 2002):

$$Bel(B) = \sum_{A \subseteq B} m(A) \tag{6}$$

The combination rules of multiple belief functions (e.g., multiple classifiers) in evidence theory are:

$$Bel(F) = \frac{1}{1-k} \sum_{i,j,l,\cdots,A_j \cap B_k \cap C_l \cdots = F} m_1(A_i) m_2(B_j) m_3(C_l) \ldots$$

$$\forall A \subset \Theta \tag{7}$$

where, F is also a nonempty of Θ, representing the class set of final computation; $m_1(A_i)$, $m_2(B_j)$, $m_3(C_l)$, … are different member classifiers with their own recognition sets, which are identical on most occasions; $k = \sum_{A_i \cap B_j \cap C_l \cdots = \phi} m_1(A_i) m_2(B_j) m_3(C_l) \ldots$ is used to represent the conflict degree among different evidences. The coefficient $1/(1 - k)$ is named as normalization factor, aiming at not assigning non-zero probability to empty set (Al-Ani and Deriche, 2002).

The classification results of each classifier are treated as evidences. We adopt the class accuracy to define the

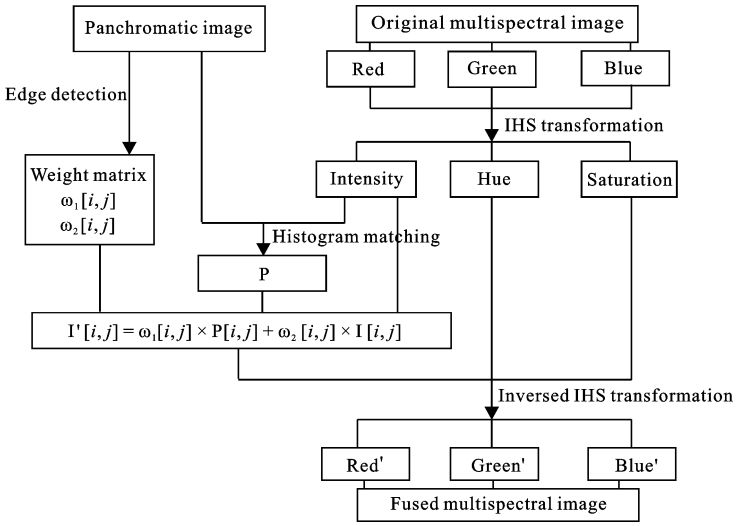

P is derived image after matching the histogram of panchromatic image with that of intensity

Fig. 1 Flowchart of improved IHS fusion using edge information from grey absolute correlation degree

basic probability allocation. For instance, when the pixel was classified by a classifier into class *i*, $m(C_i)=Q_i$, $m(\sum C_{j,j\neq i})=1-Q_i$, where Q_i is the accuracy of the class *i* by a classifier. Then evidence of each class by different classifiers is computed by Equation (7). The class label which has the highest belief function value is selected as the final class.

In order to apply D-S evidence theory to remote sensing image classification, some member classifiers should be selected to provide input evidences for combination. There are a lot of remote sensing image classifiers, for example, maximum likelihood classifier (MLC), minimum distance classifier (MDC), artificial neural network classifier (BPNN, RBFNN, and so on), decision tree classifier, and support vector machine (SVM). For a classifier ensemble, it is expected to select classifiers with high diversity and mutual complementation capacity. Based on our experiences and experiments on classifier diversity, we select MLC, MDC, and SVM to classify land cover and employ D-S fusion algorithm with three evidence inputs.

Based on statistical pattern recognition theory, MLC has been widely used to remote sensing image classification. By computing the mean spectral vector and covariance matrix for each spectral class from training samples, a decision function is generated to calculate the probability of a pixel belonging to this specific class according to Bayesian theorem. By comparing the probabilities of a pixel belonging to all classes, the pixel is then categorized into the class with the maximum probability (Richards and Jia, 2006).

MDC is another popular algorithm for classification. With this classifier, training samples are used to determine class mean vectors, and classification is then performed by assigning a pixel to the class whose mean vector has the nearest distance (Richards and Jia, 2006).

SVM is based on statistical learning theory and belongs to non-parametric classification methods. The criterion of SVM is Structural Risk Minimization (SRM). SVM classifier is able to generate a hyperplane between training samples to separate two classes in a multidimensional feature space. The optimization procedure aims at maximizing the margin between the closest training samples and the hyperplane. SVM can learn 'good' classification hyperplane in high dimension feature space. It usually outperforms traditional classifiers in terms of classification accuracy (Mathur and Foody, 2008; Waske *et al*., 2009).

Similar to our experiment and analysis, the diversity and complementation of MLC, MDC and SVM are also confirmed by Foody (2007) in their study on classifier ensemble. Therefore, an effective classifier ensemble is generated. In the next steps, MLC, MDC and SVM are used to classify remote sensing images, and their outputs are then combined by D-S evidence theory to derive a final classification result.

4 Experiment and Analysis

4.1 Study area

Xuzhou City, named as the 'coal sea of eastern China', is a typical mining industrial city. It is a large coal production site with output of raw coal more than 1.0×10^7 t each year. In this study, Pangzhuang Coal Mine, located in the northwestern of Xuzhou City is selected as the case study area. The area of this coal field is more than 18.3 km^2, and annual coal production is more than 2.6×10^6 t. The mining history of Pangzhuang Coal Mine has been more than 30 years, resulting in serious ground surface subsidence, land resource waste and regional environment degradation. Land reclamation and ecological reconstruction are being strengthened in recent years, in which remote sensing images are the most important data sources for acquiring information about land cover, land use and ecological environment.

4.2 Data

Beijing-1 small satellite, as one component of Disaster Monitoring Constellation (DMC), is equipped with two sensors that can capture multispectral images with medium resolution of 32 m and panchromatic image with high spatial resolution of 4 m (wavelength interval: 0.5–0.8 μm). Multispectral sensor consists of three bands: green (0.52–0.62 μm), red (0.63–0.69 μm) and near infrared spectrum (NIR) (0.76–0.90 μm). The satellite has advantages such as multi-resolution, high temporal resolution (3 to 5 days) and wide coverage (maximum 600 km swath).

Beijing-1 small satellite multispectral images captured on February 2, 2007 and panchromatic spectral image captured on September 10, 2007 are used in this study. After radiometric correction, image registration was done by image to image mode, and the registration error was less than 0.5 pixel. Figures 2a and 2b repre-

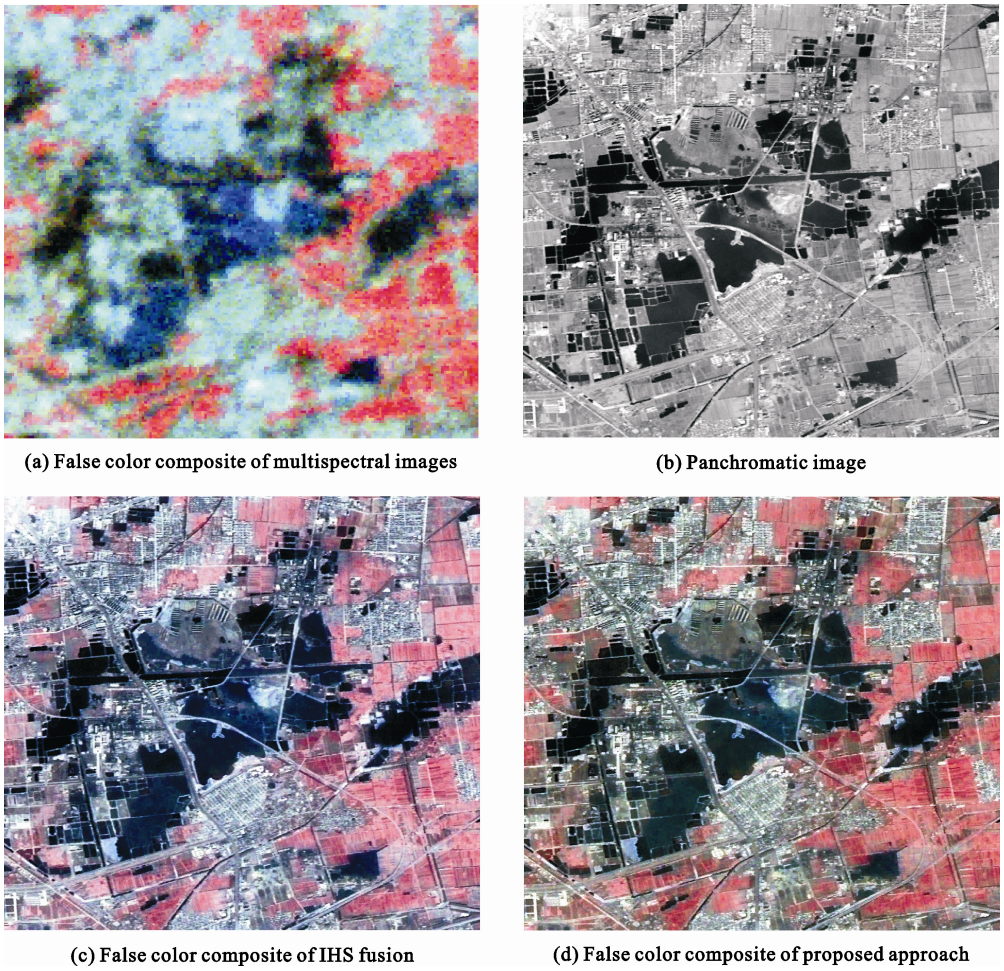

(a) False color composite of multispectral images (b) Panchromatic image

(c) False color composite of IHS fusion (d) False color composite of proposed approach

Fig. 2 Original and fused Beijing-1 remote sensing images

sent the false color composite of multispectral images and the panchromatic image used in this experiment.

4.3 Comparison of fusion methods

The improved IHS fusion algorithm mentioned above is used to fuse the panchromatic image and multispectral images. For edge detection of panchromatic image, the threshold of correlation degree is specified as 0.92 based on a comparison to the edge detection results using different thresholds. If correlation degree of a pixel to reference sequence is higher than 0.92, it is viewed as a non-edge point. Otherwise, the pixel is considered as an edge point.

In data fusion process, linear weighted summation is used to combine panchromatic image P with intensity component I after histogram matching. Based on experiments and statistical analysis, the weights are specified as 0.8 and 0.2. So the following equation is used to create a new intensity component I′.

$$I'[i,j] = \omega_1[i,j] \times P[i,j] + \omega_2[i,j] \times I[i,j] \quad (8)$$

If pixel $P[i,j]$ is an edge point, $\omega_1[i,j] = 0.8$ and $\omega_2[i,j] = 0.2$; if pixel $P[i,j]$ is a non-edge point, $\omega_1[i,j] = 0.2$ and $\omega_2[i,j] = 0.8$.

Figure 2c represents the false color composite of fused multispectral images by standard IHS fusion algorithm. In contrast, the false color composite of fused multispectral images by using the improved IHS fusion is displayed in Fig. 2d. The fusion results are qualitatively evaluated at first. In Fig. 2d, the textures and edges of road, seeper subsidence area and cropland are quite clear and visible, and the spatial resolution is improved greatly in contrast with original multispectral data (Fig. 2a). Compared with the result of conventional IHS fusion shown in Fig. 2c, the details in the fused image of this proposed method are quite similar, but it has strong spectral information preservation ability, evidenced by the close spectral signature to original multispectral images. Comparing Fig. 2a and Fig. 2c, it

can be seen that hue and color information in the fused image of IHS algorithm is greatly different from the original multispectral images, indicating serious spectral distortion and large spectral information loss. However, it is found that the spectral distortion between Fig. 2a and Fig. 2d is quite low, so the proposed fusion approach outperforms standard IHS fusion algorithm in terms of spectral information preservation capacity.

The fusion results are further qualitatively evaluated using four parameters: information entropy, average gradient, correlation coefficient and distortion index (Table 1). The entropy of the fused image by the improved IHS fusion method is higher than that of traditional IHS method, meaning the proposed approach is able to inject more information to original image owing to more introduction of high frequency information. The proposed approach gets less distortion index and higher correlation coefficient than traditional IHS algorithm, which means this approach preserve the spectral information in original multispectral images effectively. However, the average gradient of this approach is lower than that of IHS algorithm, indicating that the proposed method is weaker than standard IHS algorithm in terms of enhancing spatial resolution and injecting spatial detail, owing to the use of weights to combine intensity component with panchromatic image. But it is much higher than the average gradient of original data, demonstrating the effectiveness of fusion operation.

Based on the qualitative analysis and quantitative assessment, we conclude that the proposed fusion approach outperforms traditional IHS fusion algorithm in terms of spectral information preservation and spatial detail enhancement. Therefore, it is used to fuse the panchromatic and multispectral data of Beijing-1 small satellite for further classification and land cover change analysis.

4.4 Land cover classification

As mentioned above, three classifiers, including maximum likelihood classifier, minimum distance classifier, and support vector machine classifier, are selected as member classifiers, and D-S evidence theory is used to combine their outputs to obtain final classification results.

Considering regional properties and ground object characteristics, the land cover is categorized into 5 classes: cropland, built-up land, seeper subsidence area, public green land, and bare land. Built-up land includes residential area, industrial building and roads. Public green land also includes green space in parks, residential areas and along the roadsides.

Training and testing samples are obtained by manual interpretation and selection according to our experiences and knowledge to the study area, ancillary land cover map and other high resolution remote sensing images. After training samples are selected, SVM, MDC and MLC classification are implemented by ENVI 4.3 software, and testing samples is used to derive confusion matrix and evaluate classification accuracy. The D-S evidence classification algorithm is developed based on ENVI 4.3 and IDL 6.3. The classification results are shown in Fig. 3, and accuracy statistics is summarized in Table 2 and Table 3.

According to Table 2, different classifier gets different classification accuracy, representing different classification performance. The overall accuracy of MLC, MDC and SVM is 86.07%, 76.41% and 84.20%, respectively, and the classification accuracy increases to 87.18% by classifier combination based on D-S evidence theory. Therefore, the classification based on D-S evidence theory is able to improve overall classification accuracy of the fused multispectral images because it combines the advantages of multiple member classifiers.

From Table 3, it is found that built-up land and green space land get the low classification accuracy totally in contrast with other land cover types, which might result from mixed pixels in those areas. Classification result of MLC shows that seeper area gets the highest accuracy but built-up land gets lowest accuracy. Comparatively, result of MDC indicates that seeper subsidence area gets

Table 1 Quantitative statistics of fusion images

Image	Average gradient	Entropy	Distortion index	Correlation coefficient
Original data	2.08	4.60	–	–
Fusion image of traditional IHS method	10.29	6.09	0.54	0.58[a]
Fusion image of improved IHS method	9.16	6.62	0.43	0.60[b]

Note: a and b are the correlation coefficients between original multispectral images and fused images using different methods; '–' means no data

the highest accuracy but green space land and building area get lower accuracy. Unlike those two classifiers, result of SVM shows that cropland gets the highest accuracy but green space land and bare land get lower accuracy. It is obvious that those member classifiers have various performances to different land covers, and it is difficult to select an individual classifier that can obtain satisfactory accuracy to all classes. But this inconsistency or diversity plays important roles in classifier ensemble, so we adopt D-S evidence theory to combine the outputs of three classifiers in order to make full use of their classification capacity.

After the combination of three classifiers based on D-S evidence theory, the result shows that the overall accuracy is improved, and classification accuracy of each type is located within the interval between the highest and lowest accuracy of three member classifiers. Unlike those member classifiers that are always weak to one or more classes, the classification result of D-S evidence theory can find a quite good balance among the accuracies of all classes by combining the advantages of all member classifiers. Although the accuracy of some specific classes decreases a bit, there are not any low accuracy classes when D-S evidence theory is used. The results confirm that one classifier may perform well to certain or several land cover types in classification, but poor to other classes. In contrast, D-S evidence theory can integrate the advantages of all classifiers to improve the overall accuracy, enhance the accuracy of weak classes and ensure the stability of classification results.

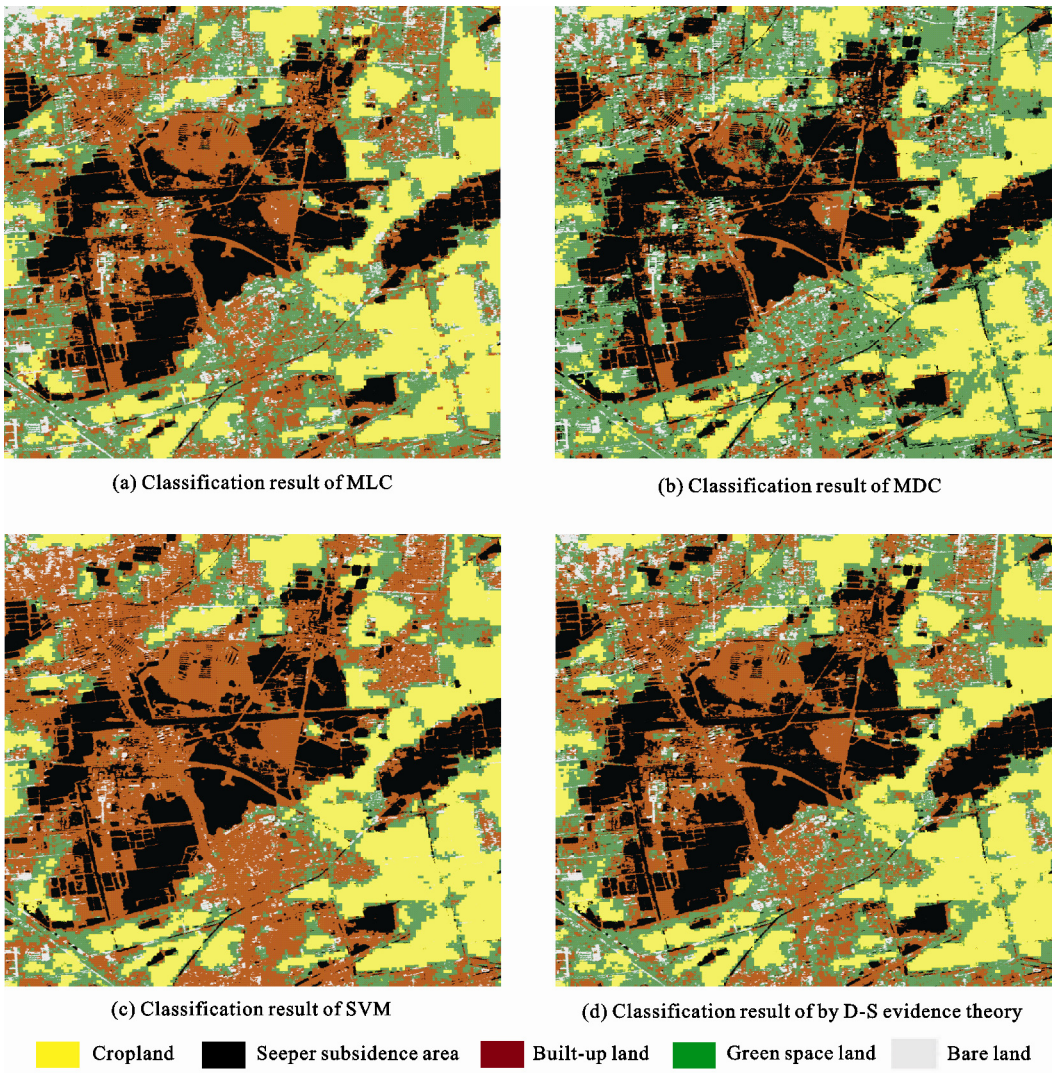

MLC: maximum likelihood classifier; MDC: minimum distance classifier; SVM: support vector machine; D-S: Dempster-Shafer

Fig. 3 Classification results from different classifiers in study area

Table 2 Classification accuracy of land cover using different methods

Classifier	Overall accuracy (%)	Kappa coefficient
MLC	86.07	0.8090
MDC	76.41	0.6788
SVM	84.20	0.8005
D-S	87.18	0.8225

Notes: MLC, maximum likelihood classifier; MDC, minimum distance classifier; SVM, support vector machine; D-S, Dempster-Shafer

Table 3 Classification accuracy for different land cover classes (%)

Land cover	MLC	MDC	SVM	D-S
Cropland	94.83	95.44	99.92	98.02
Built-up land	80.87	62.59	92.99	83.92
Seeper area	98.25	99.84	99.84	99.84
Green space land	83.65	76.79	64.06	82.08
Bare land	90.00	77.27	77.88	81.52

5 Conclusions

In this paper, the usefulness of China′s Beijing-1 small satellite remote sensing images to land resources monitoring in coal mining areas is evaluated, and an effective fusion and classification scheme is proposed by experimenting with the BJ-1 panchromatic and multispectral images over a mining area. Grey absolute correlation degree and IHS transformation are integrated to fuse the panchromatic and multispectral images from data level, and the fused images are then classified by individual classifiers and classifier ensemble based on D-S evidence theory from decision level.

Based on this study, it is concluded that: 1) Beijing-1 small satellite remote sensing images are useful to monitor and analyze land cover change and ecological environment degradation in mining areas. 2) The improved IHS fusion algorithm performs better than traditional IHS fusion algorithm because it can improve image details and information content, preserve the original spectral information and generate low spectral distortion. 3) The classifier ensemble based on D-S evidence theory is able to integrate the advantages of multiple classifiers. Therefore, the processing chain of BJ-1 panchromatic and multispectral images from data level fusion to decision level fusion is suitable to classify, monitor and analyze the land cover change in mining areas, which is expected to serve land resource monitoring, treatment and reclamation in mining areas.

However, there are still some issues needing to be addressed in the future, for example, the processing of mixed pixel in fusion process, the improvement of fusion and classification performance, and the comprehensive analysis of Beijing-1 data for ecological and environmental impacts.

References

Al-Ani A, Deriche M, 2002. A new technique for combining multiple classifiers using the Dempster-Shafer theory of evidence. *Journal of Artificial Intelligence Resear*ch, 17(1): 333–361. doi: 10.1613/jair.1026

Chen Huali, Chen Gang, Li Jinglan *et al*., 2004. RS based ecological environmental dynamic monitoring in mining area. *Resources Science*, 26(5): 132–138. (in Chinese)

Deng J L, 1997. Transformation in grey inference. *The Journal of Grey System*, 9(10): 1136–1139.

Foody G M, Boyd D S, Sanchez-Hernandez C, 2007. Mapping a specific class with an ensemble of classifiers. *International Journal of Remote Sensing*, 28(8): 1733–1746. doi: 10.1080/01431160600962566

Fu Nanxiang, Guo Ziqi, Yuan Quan, 2007. Research and implementation of multi-spectral image restoration of micro-satellite Beijing-1. *Remote Sensing Information*, 22(1): 59–62. (in Chinese)

He Guiqing, Hao Chongyang, Wang Yi *et al*., 2007. New and better image fusion method based on grey correlation analysis and IHS transform. *Application Research of Computers*, 24(7): 312–314. (in Chinese)

Kiranmay S, 2005. *Impact of Coal Mining on Vegetation*: *A case Study in Jaintia Hills District of Meghalaya*, *India*. Netherlands: International Institute for Geo-Information Science and Earth Observation.

Legg C A, 1990. Applications of remote sensing to environmental aspects of surface mining operations in the United Kingdom. In: Institution of Mining & Metallurgy. *Remote sensing*: *An Operational Technology for the Mining and Petroleum Industries*. London: Kluwer Academic Publishers, 159–164.

Li Jiong, Li Humin, Liu Xingtang, 2007. Target recognition of multi-mode compound control and guidance based on Dempster-Shafer theory. *Journal of Detection & Control*, 29(1): 76–79. (in Chinese)

Li Xuequan, 1995. Research on the computation model of grey interconnect degree. *Systems Engineering*, 13(5): 58–61. (in Chinese)

Liu Chunping, Dai Jinfang, Zhong Wen *et al*., 2003. Multiple sources data fusion using fuzzy Dempster-Shafer evidential reasoning approach to classification. *Pattern Recognition &*

Artificial Intelligence, 16(2): 213–218. (in Chinese)

Lu Feng, Liu Xiang, Liu Quan, 2000. The theory of gray relative analysis and its new research. *Journal of Wuhan University of Technology*, 22(2): 41–43. (in Chinese)

Ma Miao, Hao Chongyang, Han Peiyou *et al.*, 2004. Image fidelity criterion based on grey correlation analysis. *Journal of Computer-Aided Design and Computer Graphics*, 16(7): 978–983. (in Chinese)

Manfred E, Sascha K, Astrand P J *et al*., 2010. Multi-sensor image fusion for pansharpening in remote sensing. *International Journal of Image and Data Fusion*, 1(1): 25–45. doi: 10.1080/19479830903561985

Mathur A, Foody G M, 2008. Multiclass and binary SVM classification: Implications for training and classification users. *IEEE Geoscience and Remote Sensing Letters*, 5(2): 241–245. doi: 10.1109/LGRS.2008.915597

Mei Zhenguo, 1992. The concept and computation method of grey absolute correlation degree. *Systems Engineering*, 10(5): 43–44. (in Chinese)

Mu Fengyun, Zhang Zhengxiang, Chi Yaobin *et al*., 2007. Dynamic monitoring of built-up area in beijing during 1973–2005 based on multi-original remote sensed image. *Journal of Remote Sensing*, 11(2): 257–268. (in Chinese)

Peng Suping, Wang Lei, Meng Zhaoping *et al*., 2002. Monitoring the seeper subsidence in coal district by the remote sensing-examples from Huainan coal district. *Journal of China Coal Society*, 20(4): 374–378. (in Chinese)

Prakash A, Gupta R P, 1998. Land use mapping change detection in coal mining area——A case study in the Tharia, Coalfield, India. *International Journal of Remote Sensing*, 19(3): 391–410. doi: 10.1080/014311698216053

Rainer S, Klaus B, Marco D' E , 2010. Small satellites for global coverage: Potential and limits. *Journal of Photogrammetry and Remote Sensing*, 65(6): 492–504. doi: 10.1016/j.isprsjprs.2010.09.003

Richards J A, Jia X P, 2006. *Remote Sensing Digital Image Analysis*: *An Introduction* (*4th edition*). Berlin, Heidelberg: Springer-Verlag Berlin Heidelberg.

Shafer G, 1976. *A Mathematical Theory of Evidence*. Princeton: Princeton University Press.

Silva M P S, Camara G, Souza R C M *et al*., 2005. Mining patterns of change in remote sensing image databases. In: *Proceedings of the Fifth IEEE International Conference on Data Mining*. USA: Washington D.C.

Wang Qian, Zhang Zhenxiang, Mu Fengyun *et al*., 2007. Research on ′Beijing-1′ micro-satellite image quality and land use classification precision. *Journal of China University of Mining & Technology*, 36(3): 386–389. (in Chinese)

Wang Xuhong, Zhou Mingquan, Geng Guohua, 2004. Research of the application of the theory of Dempster-Shafer in intelligent remote sense classification. *Computer Applications and Software*, 21(9): 28–30. (in Chinese)

Waske B, Benediktsson J A, Arnason K *et al*., 2009. Mapping of hyperspectral AVIRIS data using machine learning algorithms. *Canadian Journal of Remote Sensing*, 35(supp.1): S106–S116. doi: 10.5589/m09-018

Zheng Zihua, Chen Jiazhen, Chen Liyong, 2004. An algorithm of image edge detection based on gray correlation analysis. *Journal of Fujian Normal University* (*Natural Science Edition*), 20(4): 20–23. (in Chinese)